EFDA–JET–PR(06)27

P.C. de Vries, K.M. Rantamäki, C. Giroud, E. Asp, G. Corrigan, A. Eriksson, M. de Greef, I. Jenkins, H.C.M. Knoops, P. Mantica, H. Nordman, P. Strand, T. Tala, J. Weiland, K.-D Zastrow and JET EFDA Contributors

Plasma Rotation and Momentum Transport Studies at JET

Plasma Rotation and Momentum Transport Studies at JET

P.C. de Vries[1], K.M. Rantamäki[2], C. Giroud[1], E. Asp[3], G. Corrigan[1], A. Eriksson[4], M. de Greef[5], I. Jenkins[1], H.C.M. Knoops[5], P. Mantica[6], H. Nordman[4], P. Strand[4], T. Tala[2], J. Weiland[4], K.-D Zastrow[1] and JET EFDA Contributors*

[1]*EURATOM/UKAEA Fusion Association, Culham Science Centre, Abingdon, OX14 3DB, UK.*
[2]*VTT Technical Research Centre of Finland, EURATOM-Tekes, Espoo, Finland.*
[3]*EPFL-CRPP, Association Euratom-Confédération Suisse, CH-1015 Lausanne, Switzerland.*
[4]*Chalmers University of Technology, EURATOM/VR Association, Göteborg, Sweden.*
[5]*Eindhoven University of Technology, Dept. of Applied Physics, Eindhoven, The Netherlands.*
[6]*Istituto di fisica del plasma, Associazione Euratom-ENEA-CNR, Milan, Italy.*
** See annex of J. Pamela et al, "Overview of JET Results ", (Proc. 20th IAEA Fusion Energy Conference, Vilamoura, Portugal (2004)).*

Preprint of Paper to be submitted for publication in
Plasma Physics and Controlled Fusion

ABSTRACT

An experimental study in plasma rotation and momentum transport was carried out at JET. The toroidal rotation profile was found to scale approximately with that of the ion temperature. However, significant deviations from this were found in high density ELMy H-mode discharges, which had broader rotation profiles. A rotation database analysis showed the variation of the dimensionless Mach number with respect to the plasma scenario. For predominantly NBI heated discharges the Mach number was found to be in the range of 0.3–0.45. Larger Mach numbers were observed in type I ELMy H-modes, while scenarios exhibiting type III ELMs or L-mode had lower Mach numbers. Advanced scenarios often showed a significant increase in the central Mach number when an internal transport barrier formed. A detailed study was done to investigate the Prandtl number, P_r, defined as the ratio between momentum and ion heat diffusivity. Generally the Prandtl number was found to be significantly below unity, e.g. $0.18 < P_r < 0.35$. Although it is often predicted that momentum and heat diffusivity are equal in ITG dominated plasma, also for high density ELMy H-mode discharges with temperature profiles close and above the ITG threshold, the Prandtl number was $P_r \sim 0.3$. The off-axis NBI torque in these high density discharges, and the finite gradient in the velocity profile, may indicate the presence of a momentum pinch.

1. INTRODUCTION

For ITER plasmas, with larger inertia and a lower available torque, plasma rotation is expected to be lower compared to present devices. Rotation is believed to play an important role in the suppression of turbulence in Tokamak plasmas and, therefore, may affect its performance. In order to be able to confidently extrapolate our knowledge of plasma rotation to low torque ITER scenarios, a thorough understanding of momentum transport is required.

In many devices a relationship between viscosity and ion heat transport has been observed. Previous experiments in JET [1, 2], ASDEX [3] and DIII-D [4] have shown that the momentum confinement time is often comparable to the energy confinement time. Relations between the measured angular rotation and ion temperature profiles have also been reported. This profile consistency indicates a coupling between heat diffusivity and viscosity, which can be attributed to turbulence, a common feature in fluid dynamics. For plasmas, Ion Temperature Gradient (ITG) driven turbulence theory predicts a one-to-one relationship $\chi_\phi = \chi_i$ [5, 6]. Moreover, Ref. [7] showed that for low density electron heated plasmas, with dominant Trapped Electron Modes (TEM), one also expects equal momentum and ion heat diffusivities. In many transport models, like the original Weiland model [8], there is no separate treatment of momentum diffusivity, assuming it to be equal to the ion diffusivity.

However, recent experimental analysis has shown that the momentum diffusivity can be smaller than the ion heat diffusivity and a clear one-to-one relationship does not always hold [9]. Predictive transport simulations were not always able to satisfactory reproduce the amplitude and shape of the rotation profile, when assuming the momentum diffusivity to be equal to the ion heat diffusivity. Besides the fact that turbulence may induce a coupling between heat and momentum transport, the

available free energy could also result in inward pinches. This urged us to carry out a renewed detailed study into plasma rotation and momentum transport. The experimental study on plasma rotation, that is presented here, has been carried out on JET. Neutral beam injection (NBI) is responsible for the torque on the plasma, and is the dominant source of momentum. The JET neutral beams are injected at 2 octants, each injecting 8 independent neutral beams. Half of the beam lines are injected in partly tangential direction while the others are approximately normal to the plasma. Nevertheless, each beam has a tangential component and hence is able to drive plasma rotation. For standard operations, NBI is in co-current direction. Transfer of NBI momentum to the plasma is discussed in detail in [1]. The understanding of momentum transfer to the plasma is important, because the accurate knowledge of the torque deposition profile is necessary in order to carry out momentum transport studies. Central plasma rotation velocities in excess of 200km/s have been measured during high power neutral beam injection. Discharges with additional RF heating will be treated in this paper. RF sources could be responsible for the generation of a small torque [10], but these effects are thought to be negligible compared to the dominant NBI component for the discharges reported in this paper.

The toroidal rotation velocity and ion temperature profile are measured by means of Charge Exchange Recombination Spectroscopy (CXRS), which is a well-known and proven diagnostic technique [1, 11]. The measured quantities are those of Carbon ions and in this study it is assumed that the main plasma ions have equal temperature and velocities. Especially for plasma with large pressure gradients, such as those with an Internal Transport Barrier (ITB), this assumption does not hold and the rotation profiles need to be corrected [12]. The JET CXRS diagnostic determines the rotation velocity and temperature profile at 9 radial locations. One should note that the linear velocity is not a flux function. These effects and the accuracy of the calculation of gradient lengths, important for the determination of transport coefficients, will be addressed in the summary of this paper.

The first section will present analysis of the JET rotation and momentum confinement database, and discusses the observed variations and scaling of profile characteristics and the Mach number. The database contains a selection of JET discharges (presently over 100), of which the momentum transport and rotation parameters have been analysed in detail. Firstly, the relationship between the angular rotation profile and that of the ion temperature will be discussed. Although often a strong relationship between both profiles has been reported, detailed analysis of a large number of JET discharges showed that in various cases the profiles deviate significantly. Thereafter, the plasma rotation has been characterised by the Mach number, a dimensionless parameter, which eases comparison between various JET scenarios and also with other devices. The characteristic Mach number for both ELMy H-mode discharges and those with ITBs will be given. Variations in the central Mach number, or the Mach profile in general, can be due to differences in the torque and heat deposition profile. However, another, more important, factor may be the momentum and heat transport.

After this detailed analysis of the profiles, the energy and momentum sources will be treated and the local transport properties, the ion heat and momentum diffusivities will be calculated. The so-

called Prandtl-number, which is defined as the ratio between the momentum and ion heat diffusivity: $P_r = \chi_\phi / \chi_i$, is determined in section 3. This study is focused particularly on type I ELMy H-mode discharges. Because of the complications with the determination of the bulk ion rotation profile and its gradient, in the presence of strong ITBs, these discharges have been left out of this analysis. Both interpretative studies by means of the JETTO code [13], and analysis with the Weiland-model [8] have been carried out. In section 3 the global confinement of momentum and energy of these discharges will be described. It will be shown that although the momentum diffusivity in the plasma gradient region is much smaller than the ion heat diffusivity, the global confinement of momentum and energy can be similar. The paper concludes with a summary.

2. ROTATION AND TEMPERATURE PROFILES

The observation of profile consistency between the ion temperature and angular rotation has been reported in many devices. Here, the ratio of the angular rotation and ion temperature determined from each of the CXRS channels, have been analysed. This ratio will indicate a coupling between the local temperature and rotation. The variation from channel to channel may reveal profile differences. A statistical analysis over a large number of discharges has been carried out. A similar analysis was carried out on DIII-D CXRS data [4].

The first inner most CXRS channel, measures at R_1 ~ 3.2m, while the geometrical radius of the JET torus is Ro=2.96m. The other consecutive channels are located further outwards at intervals of approximately 0.1m and R7"<3.8m. The two outer most channels have been omitted from this study. Discharges have been selected from the period 2000-2004, of which the first group consisted of approximately 850 discharges that featured optimised or reversed magnetic shear and in many cases internal transport barriers, while the second group, of approximately 1090 discharges, consisted of ELMy H-modes.

The statistical analysis, shown in figure 1a, reveals that for ITB discharges, there is little variation in the ratio between the local angular rotation frequency and ion temperature, ω/T. The average value of the central channel (at $R_1 = 3.2$m) is found to be: $\omega/T = 9.0 \pm 2.5$ rad/eVs. The average values for the other channels are shown in table 1. Generally, all channels show the same ratio within the spread of the data, although, one might say that the value of the outer channel is slightly higher. This shows that for ITB discharges in JET the angular rotation profile matches that of the ion temperature. This can be further illustrated by an example discharge, shown in figure 2. When the internal transport barrier forms, both the rotation and ion temperature increase. Beside an increase in velocity, an increase in total momentum was found. Since the momentum input remained constant, it indicates that both the ion energy and momentum confinement improve with the formation of the ITB. The ratio ω/T is shown for the 7 different radial positions, and seem to be unaffected by the formation of the barrier. Thus, although the transport is reduced with the formation of the barrier, the ratio of momentum and heat transport is expected to be unaffected for this discharge. This is an indication that both the momentum and

ion temperature are similarly affected in a by the suppression of turbulence and formation of the ITB.

A different picture is found when doing the same exercise for H-mode discharges. In figure 1b, one clearly sees that, firstly, the variation in the value of ω/T for each channel is larger, while also the average values are significantly larger than those for ITB discharges. Only at the central channel, the distribution peak that matches the values found for ITBs. However, the average value for this channel was found to be larger: $\omega/T = 13.6 \pm 3.6$ rad/eVs. The average value of ω/T increases for those channels that are further outward. This shows that for this set of discharges, profile consistency does not hold.

There are several indications that the ratio ω/T is affected by the density, e.g. at higher densities the ratio is larger at the edge. Comparably, the ITB discharges are often done at much lower density than H-mode discharges. For a large set of ELMy H-mode discharges the scaling of ω with T gave $\omega/T\ 1^{-\alpha}$=constant with $\alpha \approx$H0.2-0.4. Furthermore, discharges with a larger fraction of ICRH power showed smaller values of ω/T. This will also be reflected in the Mach number as shown hereafter. A Type I ELMy H-mode discharge, in figure 3, clearly shows larger values of ω/T for the edge CXRS channels. However, a back-transition to L-mode at t≈H15.75s, leads to a reduction of ω/T at the outer channels, while also the scatter between channels is much smaller. Note, that the back transition results in a lower line-averaged density. At t≈H16.3s the plasma returns to H-mode, yielding an increase in density and the edge ratio of ω/T. Proper type I ELMy H-mode starts at t≈H17s.

2.1 GRADIENT LENGTHS OF THE ROTATION PROFILE

The fact that the rotation and ion temperature profiles deviate for certain JET scenarios, may indicate that the heat and momentum diffusivities are not equal in these cases. An accurate determination of these quantities is not easy. Complications arise from the accuracy with which one can determine the profile gradients, due to the limited amount of data points (9 CXRS channels) and the error associated with each measurement point (approximately 10%). In order to take these errors into account when calculating the gradients, a smooth fit was applied to the plasma profiles. To reduce the error, profiles were averaged over a steady state plasma phase of ~ 0.2s. The measured profiles of both parameters are mapped on poloidal $\sqrt{\psi}$ co-ordinates.

The inverse normalised gradient length R/L is defined as the derivative of the natural logarithm of the profile, normalised to the major radius. These gradient lengths of both the ion temperature and rotation velocity profiles, R/L_T and R/L_v, respectively, have been determined for ELMy H-mode discharges in the JET momentum database. Note, that the velocity and not angular frequency profile is used. In large aspect ratio approximation, both profiles can be assumed equal, and the error made with this approximation is still smaller than the measurement error. In figure 4, the local gradient lengths for these profiles have been plotted against each other. The inverse gradient lengths of the rotation profile are smaller than those of the temperature profile. A similar observation was made in AUG [9]. In the next section the gradient length of the momentum density profile will be discussed.

2.2 MACH NUMBER OF JET PLASMAS

The dimensionless Mach number can be used to compare plasma rotation in various devices or different plasma scenarios. The Mach number is defined as ratio of the kinetic and thermal speed of the plasma species:

$$M \equiv \frac{v_{kin}}{v_{therm}} = \sqrt{\frac{m}{e}} \frac{v}{\sqrt{T}} \qquad (1)$$

Here, the m is the mass of the species and v its (toroidal) rotation velocity in [m/s]. The temperature, T, is given in [eV]. The Mach number gives the square root ratio of the kinetic energy and the thermal energy. It depends both on the ratio of torque and heating power and the ratio of heat and momentum confinement. The Mach numbers given in this paper are for Deuterium ions under the assumption that the Deuterium rotation velocity and temperature are equal to those measured for Carbon.

The NBI torque and heat deposition are linked. Hence, in the presence of a strong coupling of momentum and heat transport, one expects little variation in the Mach numbers of purely NBI heated plasmas. Analysis of NBI-only (ELMy H-mode) discharges shows that these have a central Mach number of M=0.4. Note that these values are for the Deuterium ions, while the Mach number for Carbon is a factor $\sqrt{(m_C/m_D)} \approx 2.4$ larger. Carbon Mach numbers are found to be above unity for many JET discharges. Similar values have also been found in other devices, see for example Ref. [14].

Figure 5 shows the central Mach number for the bulk Deuterium ions for different scenarios with a mixture of NBI and ICRH auxiliary heating. The first observation is that the Mach number for each of the 3 scenarios decreases with the fraction of NBI power. A larger fraction of ICRH power, results in a lower Mach number. If one assumes ICRH is able to increase the temperature, without applying significant torque, it can explain that the Mach number decreases with larger ICRH power fractions.

Furthermore, a difference in the average Mach number between L-mode, Type III, Type I ELMy H-modes and discharges with ITBs can be seen. Each group, respectively, has higher central Mach numbers. This can be explained by the difference in temperature between H-mode and ITB discharges. In the previous section it has been shown that the angular rotation frequency scales approximately with the temperature, or the ratio of ω/T or v/T is approximately (not exactly) constant. Because the Mach number scales with v/”T, higher temperatures result in larger Mach numbers. This can also been seen in figure 2: the Mach number increases together with the central temperature when the ITB forms. ITB discharges in JET feature rather large central Mach number of the order of M=0.5-0.65. Figure 3 shows that the HL back-transition does not affect the central Mach number, which stays constant through the transitions. However, a clear change in the outer Mach number is observed, which are generally larger for H-mode than for L-mode.

For H-mode discharges the Mach profile is flatter than that for L-mode discharges. In figure 3, one sees a decrease of the outer Mach number with the transition from H to L-mode. Because the

Mach number scales with v/”T, one finds for its gradient length:

$$R/L_M = R/L_v - 2R/L_T \tag{2}$$

For ELMy H-mode discharges, rotation profiles are broader with larger gradient lengths (i.e. smaller R/Lv) compared to ion temperature profiles. Broader rotation profiles will also result in a larger ratio of Ö/T, which we already found in the previous section. The transition from L to H-mode obviously causes a broadening of the rotation profile.

3. HEAT AND MOMENTUM TRANSPORT

In the previous section it was shown that, although the ion temperature and toroidal rotation profiles are similar, significant variations are found, especially in high density discharges. The question arises whether these variations are due to different transport properties. At high density, the rotation profiles are broader than those of the ion temperature, which may seem to indicate that momentum diffusion is larger. However, one should also consider differences in the source profiles. The momentum and ion heat source are linked but not necessarily identical. As we will see later in this section, the torque and ion heat deposition profiles applied by NBI can differ significantly. NBI delivers its torque to the main ions, while it may heat these ions only partly, with another portion going to the electrons. Non-diffusive losses are also difficult to interpret and are included in the total effective diffusivities. In this section, heat and momentum transport in ELMy H-mode JET discharges will be analysed. In order to determine the effective momentum and heat diffusivities both the gradient lengths of the profiles as well as the sources should be determined. Both diffusivities are defined as:

$$Q_i = n_i \chi_i^{eff} \nabla T_i \tag{3}$$

$$S_\phi = \chi_\phi^{eff} \nabla \Omega \tag{4}$$

where Q_i and ni are the ion heat flux and density, while similarly as the heat flux, S_ϕ is the torque per surface area, or ‘torque flux’. The angular momentum density is given by Ω. Beside the accuracy of the gradient lengths, the determination of the heat and momentum diffusivities can be affected by subtle differences in the calculated torque and heat deposition profile.

For detailed analysis of the diffusivities and their ratio, a series of type I ELMy H-mode discharges has been selected with the properties: a large density profile gradient length or $R/L_n<0.2$ and, equal electron and ion temperatures, $T_e \approx T_i$. For these conditions, ITG turbulence is expected to be the dominant turbulent mode [15]. These criteria also reduce complications with additional heat loss channels, such as ion-electron exchanges. The line averaged density of these discharges was of the order of $n_e \sim 2 \cdot 10^{20}\ m^{-2}$. Besides dominant NBI heating, a small fraction of on-axis ICRH (between 0-20% of the total heating power) was applied to these plasmas. The heat and momentum diffusivities

(or their ratio) can be calculated directly according to eq. (3) and (4) or by means of the interpretive simulations with the JETTO transport code [13], which includes the determination of the NBI torque and ion heat deposition by PENCIL [16] and uses measured plasma profiles as input.

These comparable discharges differed in the ion temperature gradient length R/L_T: from low gradient lengths $R/L_T \approx 3$ to those that where close to or above the ITG threshold $R/L_T \approx 5$ (see Ref. [15]). Linear gyro-kinetic analysis of the micro-turbulence by means of the KINEZERO code [17] showed that ITG was the dominant mode in these discharge, with increased growth rates for those closer to the critical gradient $R/L_T \approx 5$. For the latter discharges, stiff ion temperature profiles were found, with characteristic triangular profiles, while for the other discharges the profile was more parabolic.

As has been shown in the previous section the gradient of the rotation and temperature profile are not always equal. For this series of discharges, the normalised inverse gradient lengths R/L_T, R/L_v and R/L_Ω, for the gradient region of the plasma ($0.2<\rho<0.7$), have been determined. Again it was found that generally: $R/L_T > R/L_v$. In figure 6 the inverse ion temperature gradient length is plotted against the inverse momentum density gradient length R/L_Ω. Generally one could say that $R/L_T \sim R/L_\Omega$. However, because of ion temperature profile stiffness, R/L_T reaches the threshold limit, while R/L_Ω increases further. No threshold for the rotation profile gradient was found within this series of discharges. Note that the difference between R/L_v and R/L_Ω is determined by the gradient length of the (mass) density profile R/L_n which is small but not negligible.

3.1 TORQUE AND HEAT DEPOSITION

In order to calculate the momentum and heat diffusivities one has to determine heat and torque flux. The total heat deposition by NBI/ICRH and the NBI torque were computed. The NBI heat and torque deposition was determined using the PENCIL code [16]. For the series of high density H-mode discharges, the ICRH power was deposited on-axis. Although it is often stated that the total torque applied by the NBI is proportional to the input power, this does not necessarily mean that the local heat deposition to the ions should be proportional to that of the torque deposition.

The fraction of the NBI power that is transferred to the ions depends on the local temperature (e.g. collisionality). At high temperature, or low density, more NBI power will go to the ions. Hence, the ion heat deposition is generally peaked on-axis, while that of the electrons is off-axis, especially for high density discharges. At high densities the ion heat deposition profiles are generally peaked while the torque deposition profiles are hollow. As expected for ITER plasmas, a large part of the torque is deposited at the outer part of the plasma, as shown in figure 7. The observation that rotation profiles are broader than ion temperature profiles for high density plasmas, as shown in section 1, can be explained by this off-axis torque deposition.

If the average density increases, less torque is deposited in the plasma core, however, also the power fraction that is transferred to the ions decreases. It was found that the ratio of normalised torque flux (S_ϕ/Ω) and ion heat flux (Q_i/n_iT_i) did not change too much with density, but was always below unity (~0.4).

3.2 THE PRANDTL NUMBER

The ratio of both equations (3) and (4) gives the Prandtl number, which can be rewritten as:

$$P_r \equiv \frac{\chi_\phi}{\chi_i} = \frac{S_\varphi}{Q_i}\,\frac{n_i T_i}{\Omega}\left(\frac{R/L_T}{R/L_\Omega}\right) \tag{5}$$

where, R/L_T and R/L_Ω are the local normalised inverse gradient lengths of the temperature and momentum density. For the series of high density discharges, discussed above, the Prandtl number has been determined. Firstly, it has already been shown that the ratio of ion temperature and momentum density gradient length is around or just below unity (see figure 6). Furthermore, mainly because part of the NBI power is transferred to the electrons, and partly because of the hollow torque deposition at high density, the normalised ratio of torque and heat flux is also below unity (~0.4). The Prandtl numbers found for this series of discharges was in the range of $0.18 < P_r < 0.35$, which is significantly below unity. Note that these discharges were chosen to have dominant ITG turbulence, with often stiff temperature profiles. The low Prandtl numbers contradict the assumption typically used in ITER rotation predictions that $\chi_\phi/\chi_i = 1$. Because the effective ion heat diffusivity increased for discharges that were closest to the ITG threshold,

these were also found to have the lowest Prandtl number. This is supported by figure 6, which shows that the threshold did not seem to affect the momentum density gradient.

Beside the high density ITG dominated H-mode discharges, the averaged diffusivities for other discharges in the JET rotation database have been determined, as shown in figure 8. The high density discharges, discussed above, are shown in red. Other H-mode discharges that have been analysed have been added in black. The graph shows that there is a relationship between the ion heat and momentum diffusivity. However, the average Prandtl number, or ratio between the two diffusivities, is below unity: $P_r \sim 0.2$.

3.3 MODELLING OF MOMENTUM TRANSPORT

The ion heat diffusivity has been calculated self-consistently using the Weiland-model [8] for the high density ELMy H-mode discharges. The model reproduced the measured ion temperature profiles quite well. Initially, it was assumed that the momentum diffusivity equals that of the ion heat diffusivity. However, in this case the modelled rotation profiles did not fit those obtained empirically. In order to match the rotation profiles, the momentum diffusivity had to be reduced. When the momentum diffusivity was assumed to be of the order of 0.2-0.3 times the ion heat diffusivity, the model reproduced toroidal rotation velocities closest to those measured experimentally. This result confirms the empirical Prandtl numbers, shown in figure 8. However, an exact match to the experimental rotation profile proved to be difficult, indicating that beside a quantitative difference between the ion heat and momentum diffusivities, the radial profiles of these parameters may be different too. This shows the need for plasma models with a fully self-consistent calculation of momentum diffusivity [20].

4. GLOBAL CONFINEMENT OF MOMENTUM AND ENERGY

As has been shown in figure 8, the ratio between the ion heat and momentum diffusivity is constant over a large range, hence, both momentum transport and ion energy transport are clearly linked. Momentum transport in the gradient region is smaller than that of ion energy. The question arises how this is reflected in the global momentum and energy confinement. These properties can be characterised by the momentum and energy confinement times. For steady state plasmas the momentum confinement time is defined as the total toroidal angular momentum divided by the torque. It is often reported that the global confinement times of momentum and energy are equal in Tokamak plasmas [2, 3, 4].

The momentum confinement time has been calculated for a large number of discharges from the period 2000-2004, where appropriate data of plasma rotation and torque input were available. Further selection criteria were a minimum plasma current of 2MA and sufficient NBI power: P_{NBI}>6MW. However, the data set, of more than 1000 pulses, contained various plasma operation modes, such as L-mode, H-mode, Hybrid and discharges with optimised shear and ITBs. In figure 9, the ratio of the energy confinement time to the momentum confinement time is plotted against the line integrated density. At low density ($n = 5 \cdot 10^{19}\ m^{-2}$) the energy confinement time is found to be 2 to 3 times larger than the momentum confinement time. The high density tail of the data-set contains predominantly H-mode discharges, for which the momentum confinement time is similar to that of the energy.

Momentum confinement is linked to that of the ion energy and at low density clearly the electron and ion confinement/transport differ. In figure 10 the momentum confinement time is plotted against the ion energy replacement time, which is defined as ratio of the ion energy to the power to the ions. The latter parameter is derived from the NBI and ICRH ion heat deposition. The transfer of energy from the electrons to the ions has been omitted and one should be aware that this factor may me significant for discharges where $T_e \neq T_i$. A much better scaling is found with the ion energy replacement time (blue).

From figure 10, it is clear that the global momentum confinement time is similar to the ion energy replacement time. A more accurate calculation of these quantities has been done for the high density H-mode discharges discussed in the previous section. These discharges had equal electron and ion temperatures. The momentum confinement time was found to be equal to that of the ion energy confinement. This result confirms earlier observations made at JET [2]. For low density plasmas, the momentum confinement time was found to be slightly larger than that of the ion energy. Because of the better electron energy confinement in these discharges, the electron energy fraction was generally larger. Because of the omission of the electron-ion transfer power, the ion energy confinement time would have been under estimated for these low density discharges. One should note that the ratio of both global confinement times does not reflect the ratio of the local momentum and heat diffusivities. If the diffusivities were constant as a function of radius, and the rotation profile equals that of the ion temperature, both ratios should be equal. However, as has been pointed out in

section 1, the profile consistency between plasma rotation and ion temperature does not always hold, especially for high density H-mode plasmas. Furthermore, it may indicate that although the momentum diffusivity is smaller than the heat diffusivity in the gradient region of the plasma, in the edge, momentum confinement may be worse.

SUMMARY AND CONCLUSIONS

In the first section the ratio between angular momentum and the temperature was discussed. The Mach numbers of typical JET discharges for various scenarios were shown. Mach numbers showed to be higher for low density, high temperature plasmas, like those with internal transport barriers. The Mach number decreased with increasing fraction of ICRH power. For pre-dominantly NBI heated ELMy H-modes, the Mach number for the main ion species was found to be in the order of M=0.4. The dominant NBI fraction made that in most JET discharges the heating and torque sources are coupled. Nevertheless, the torque and ion heat deposition profiles can still vary significantly. Profile analysis suggested that for JET plasmas, a coupling between the rotation and ion temperature profile did not always hold. Especially, for high density H-mode discharges, the rotation and temperature profile shapes were found to deviate. This could be explained by the off-axis nature of the NBI torque deposition at high density, while the ion heat deposition is largest in the core of the plasma. Although, the torque deposition was off-axis, still a significant gradient in the momentum profile was sustained.

The ion heat diffusivity in the gradient region of the plasma was always found to be larger than the momentum diffusivity. One should note that these are effective diffusivities, hence also include convective transport. Prandtl numbers in the order of $0.18 < P_r < 0.35$ were determined. The lowest Prandl numbers $P_r \sim 0.18$ were found for high density, ITG dominated plasmas. However, even in low density plasmas, like those with internal transport barriers the Prandtl number was below unity. Earlier transport analysis of TFTR limiter discharges had obtained much higher ratios of momentum to ion heat diffusivity [18]. While analysis of AUG plasmas indicate similar Prandtl numbers as those found in this study [9].

Neo-classical theory predicts a momentum diffusivity two orders of magnitude lower than the ion heat diffusivity: $P_r \sim O(10^{-2})$ [19]. The measured Prandtl numbers in JET plasmas are significantly higher. However, the experimental values do not confirm the strong coupling given by ITG or TEM theory [5, 6, 7] and discharges closer to the ITG threshold were found to have even smaller Prandtl numbers. These results contradict the usual assumption for ITER rotation predictions ($\chi_\phi = \chi_i$) A clear trend or scaling for the Prandtl number in the core of JET plasmas could not yet be distinguished. One should remember that the error of the Prandtl numbers, obtained by this experimental analysis, is large. The error in determining the momentum and heat diffusivities is of the order of 15%, largely due to the determination of the profile gradients, and furthermore, due to uncertainties in the ion density profile and Z_{eff}. The error in the Prandlt number is estimated to be 20-25%.

For low density discharges, the ion energy and momentum confinement times could be a factor of 2-3 times smaller than the total energy confinement time. It was shown that the global confinement of momentum and ion energy scaled proportionally for JET discharges.

The fact that these global parameters are similar does not necessarily mean that the ratio of local transport properties should be unity. However, it suggests that although the momentum confinement in the core is better compared to that of the ion energy (i.e. Prandtl number is smaller than unity), this may be reversed at the edge of the plasma. The impact of, for example, the pedestal on momentum and ion energy confinement was already illustrated in ref. [1] which showed that in ELM free phases the ion energy confinement time was larger than that of the momentum.

The momentum diffusivities discussed in this report were effective values, which include convective fluxes. The possible presence of a momentum pinch has been proposed to understand the large momentum density gradients in the presence of an off-axis torque profile. However, experimental evidence for such a pinch is so-far inconclusive. Further understanding of the coupling between toroidal momentum and heat transport is required. Previously, in various plasma modes, a one-to-one relationship between ion heat and momentum diffusivity was assumed. Recently, self-consistent modelling of the momentum transport, independent from that of heat diffusivity, has been preformed, which will be reported in further publications [20].

ACKNOWLEDGEMENTS

The authors would like to acknowledge A. Thyagaraja and P. Herlander for their support and help with the understanding of plasma rotation. Furthermore, we like to thank E. Trier for his part of the database analysis. This research has been performed under the European Fusion Development Agreement and was partly funded by the UKAEA, the Physical Sciences Research Council and by the European Communities under contract of association between EURATOM and UKAEA. The views and opinions expressed herin do not necessarily reflect those of the European Commission.

REFERENCES

[1]. K.-D. Zastrow, et al., Nucl. Fusion **38** (1998) 257.
[2]. K.-D. Zastrow, et al., Proc. of the 22nd Euro. Conf. on Controlled Fusion and Plasma Physics (Bournemouth, 1995) Vol. 19C (Geneva,: European Physical Society) p453.
[3]. A. Kallenbach, et al., Nucl. Fusion **33** (1991) 595.
[4]. J.S. deGrassie, et al, Nucl. Fusion **43** (2003) 142.
[5]. N. Mattor and P Diamond, Phys. Fluids **31** (1988) 1180.
[6]. N. Mattor and P Diamond, Phys. Fluids **B 1** (1989) 1993.
[7]. A.G. Peeters and C. Angioni, Phys. Plasmas **12** (2005).
[8]. J. Weiland, A. B. Jarmen, and H. Nordman, Nucl. Fusion **29** (1989) 1810.
[9]. D. Nishijima, et al., Plasma Phys. Contr. Fusion **47** (2005) 89.
[10]. J.-M. Noterdaeme, et al., Nucl. Fusion **43** (2003) 274.

[11]. H. Weisen, et al., Nucl. Fusion **29** (1989) 2187.
[12]. D. Testa, et al., Phys. Plasmas **9** (2002) 243.
[13]. Cenacchi and A. Taroni, in Proc. of the 8th Computational Physics, Computing in Plasma Physics (Petit-Lancy, 1986) Vol. 10D, p57 (Geneva,: European Physical Society).
[14]. L.R. Baylor, et al., Phys. Plasmas **11** (2004) 3100.
[15]. X Garbet et al., Plasma Phys. Contr. Fusion **46** (2004) 1351.
[16]. C.D. Challis et al, Nucl. Fusion **29** (1989) 563.
[17]. C. Bourdelle, et al., Nucl. Fusion **42** (2002) 892.
[18]. S.D. Scott, et al., Phys. Rev. Lett. **63** (1990) 531.
[19]. F.L. Hinton and S.K. Wong, Phys. Fluids **28** (1985) 3082.
[20]. J. Weiland, et al., Proc. of the 33rd Euro. Conf. on Controlled Fusion and Plasma Physics (Rome, 2006) (Geneva,: European Physical Society)(2006).

		'ITB'		**'H-mode'**	
Channel	R (m)	ω/T (rad/eVs)	±	ω/T (rad/eVs)	±
1	3.20	19.03	2.5	13.62	3.6
2	3.35	8.42	1.8	14.54	3.3
3	3.42	8.26	2.1	15.09	3.9
4	3.57	8.34	2.0	14.47	3.7
5	3.64	9.04	2.8	15.22	3.0
6	3.71	9.05	2.5	15.26	4.9
7	3.78	9.39	2.8	16.08	5.0

JG07.10-11c

Table 1: Ratio of the average angular rotation frequency and ion temperature for the 7 inner most CXRS channels. The two columns represent the data for ITB and H-mode discharges shown in figure 1(a) and (b), respectively.

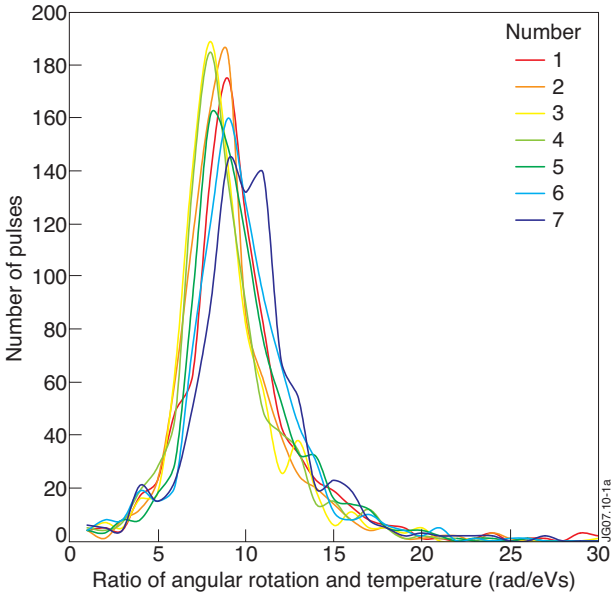

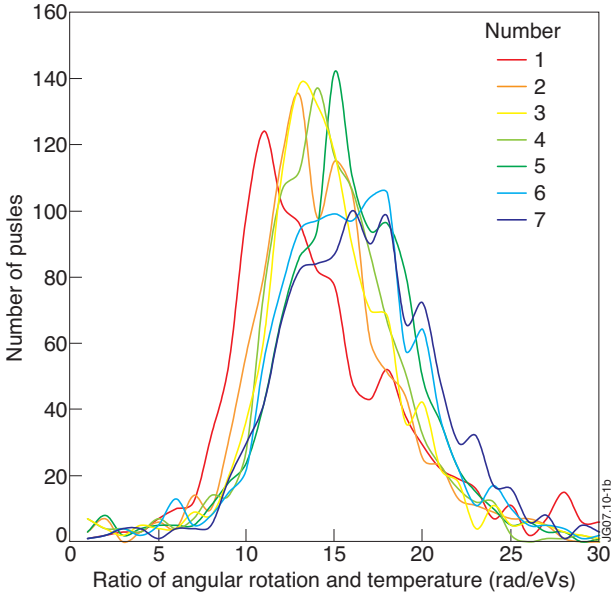

Figure 1: Statistical analysis of the ratio between the angular rotation frequency and the ion temperature, measured by 7 consecutive CXRS channels (see Table 1). a) For discharges with optimised shear and internal transport barriers. b) For H-mode discharges.

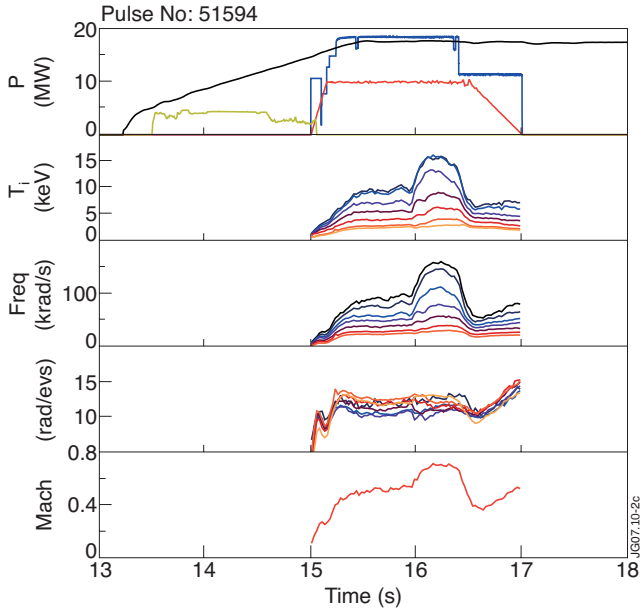

Figure 2: Example of a JET Pulse No: 51594 that forms an internal transport barrier at t=5.86s. (a) Shows a typical optimised shear discharge sequence, with LHCD heating during the current ramp phase, and a start of the main heating (NBI (blue) and ICRH (red) just prior to the start of the flat-top. (b) and (c) show the ion temperature and angular rotation frequency, respectively, measured by the 7 CXRS channels (at the positions shown in table 1). (c) The ratio of the angular rotation frequency and ion temperature at the respective positions. d) The central Mach number (red).

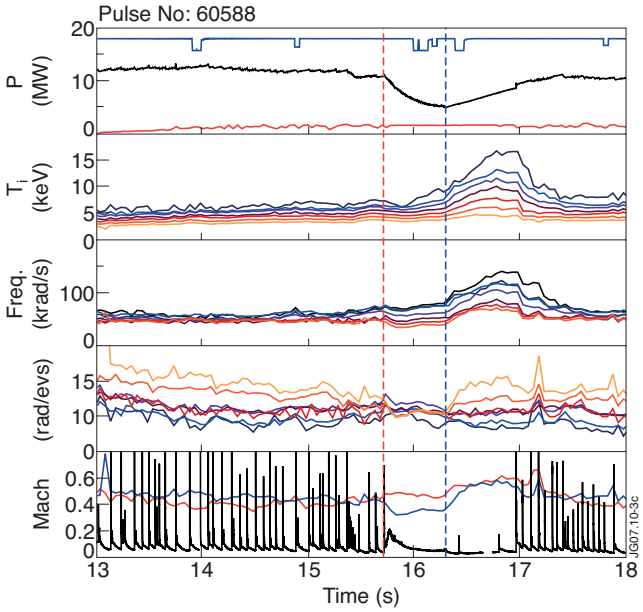

Figure 3: Example of a JET discharge (Pulse No: 60588) with an HL back-transition at t"H15.75s, and a return to H-mode at t≈H16.3s. (a) Shows the injected auxiliary heating (NBI (red) and ICRH (blue) and in black the line-integrated density in (a.u.). (b) and (c) show the ion temperature and angular rotation frequency, respectively, measured by the 7 CXRS channels (at the positions shown in table 1). c) The ratio of the angular rotation frequency and ion temperature at the respective positions. (d) The central Mach number (red) and that at the edge (blue) (R=3.7m). The D_α signal shows the ELMs in this discharge. The vertical red line shows the time of the H to L-mode transition, while the vertical blue line indicates the return to H-mode.

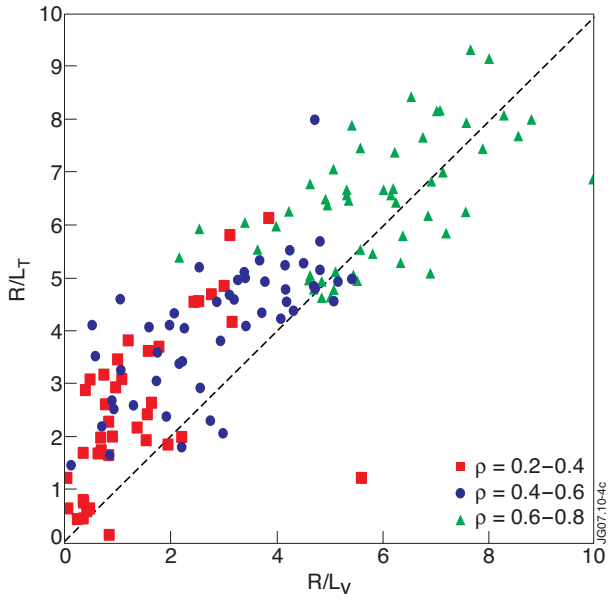

Figure 4: The rotation and temperature profile normalised gradient lengths, calculated for a series of ELMy H-mode discharges. The gradient lengths are determined in 3 plasma regions: the core (0.2<ρ<0.4) (red squares), gradient region (0.4<ρ<0.6)(blue circles) and edge (0.6<ρ<0.8) (green triangles).

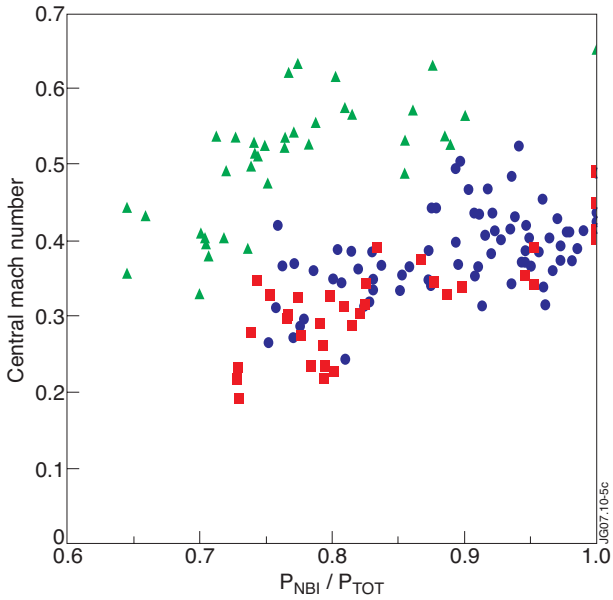

Figure 5: The central Mach number plotted as a function of the fraction of NBI power. The green triangles represent discharges with an ITB, while the red squares and the blue points, are type III and type I ELMy H-mode discharges, respectively.

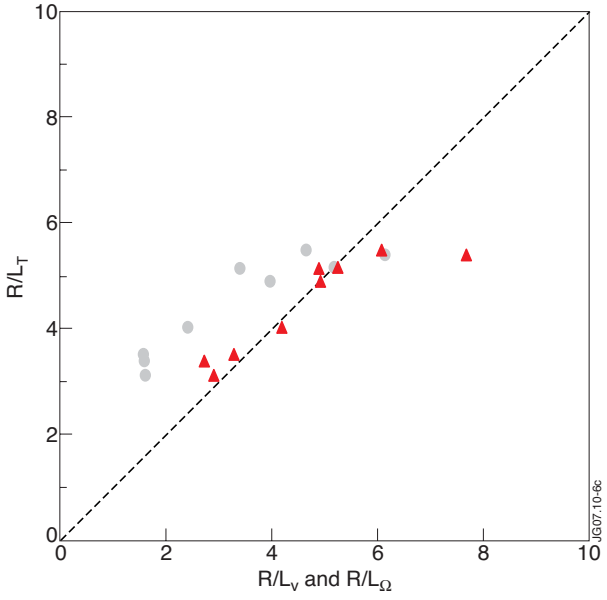

Figure 6: In red (triangles): the inverse normalised gradient length for the ion temperature profile R/L_T, plotted against that of the momentum density R/L_Ω. In some cases the momentum density gradient is larger than that of the ion temperature. In grey (dots): R/L_T is plotted against the inverse velocity gradient length R/L_v, to compare with figure 4.

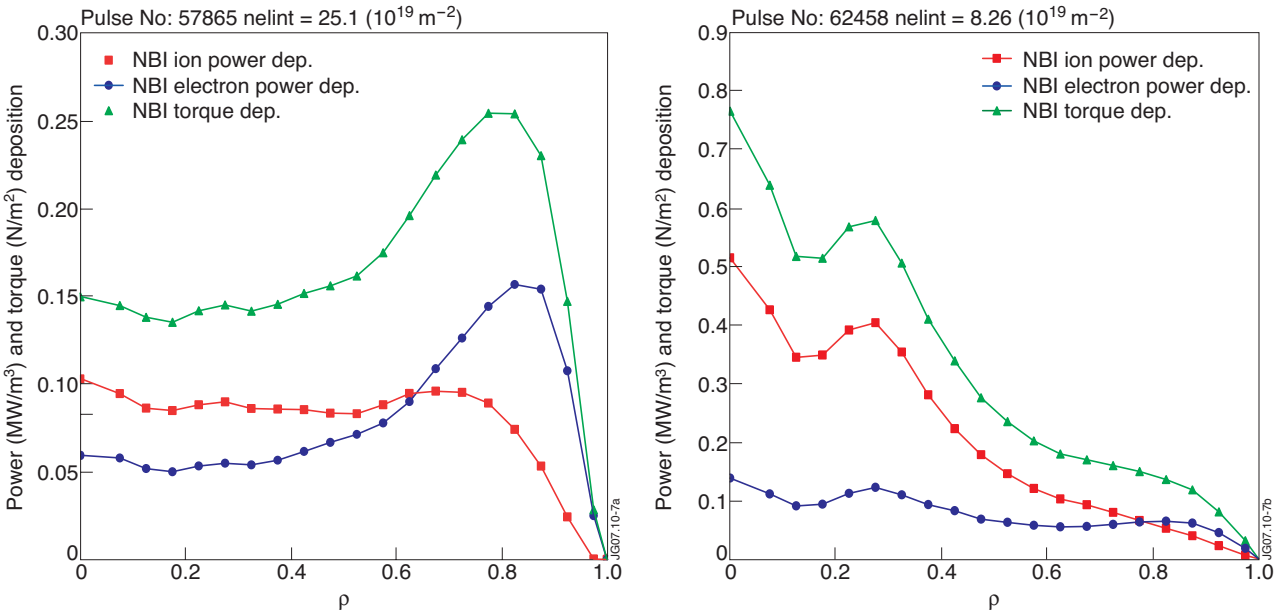

Figure 7: Deposition of ion and electron power deposition by NBI as calculated by PENCIL for two discharges with line-average densities of 8.25×10^{19} m^{-2} and 25.1×10^{19} m^{-2}, respectively. The NBI torque deposition profile is also given and shows to be hollow for the high density discharge.

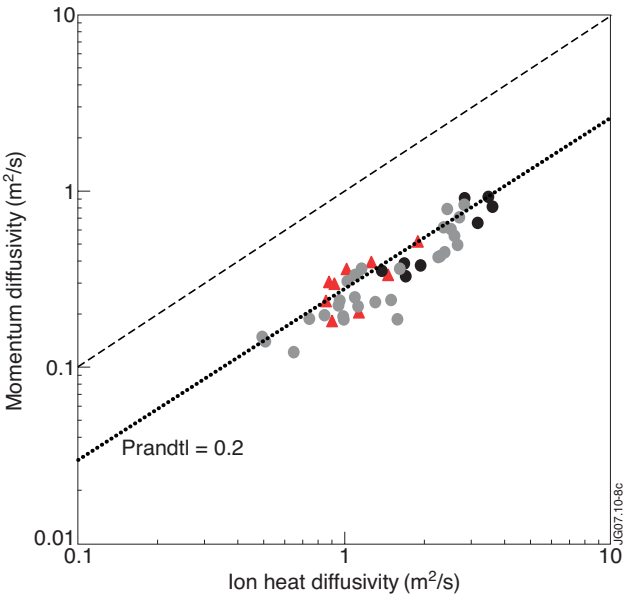

Figure 8: The momentum diffusivity as a function of the ion heat diffusivity averaged over the gradient region ($0.3<\rho<0.7$). The high density ELMy H-mode discharges from figure 6 are shown in red triangles. Other H-mode discharges are included in black (with $T_e \neq T_i$) and grey (with $T_e \neq T_i$). The error bars on both diffusivities is of the order of 15%.

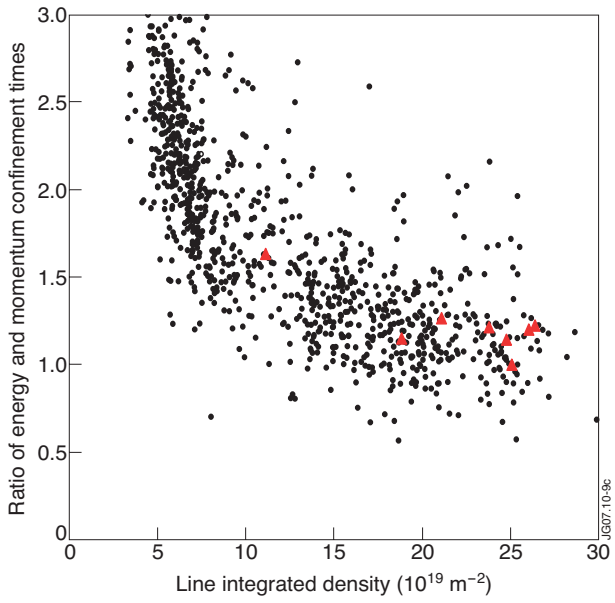

Figure 9: The ratio of the energy confinement time to the momentum confinement time as a function of line integrated density. Determined for all types of discharges (Optimised Shear/ITB, L-mode, H-mode, Hybrid) in the period 2000-2004, with $P_{NBI}>6MW$, $I_p>2MA$. In red triangles are shown the high density ELMy H-mode discharges discussed in section 3.

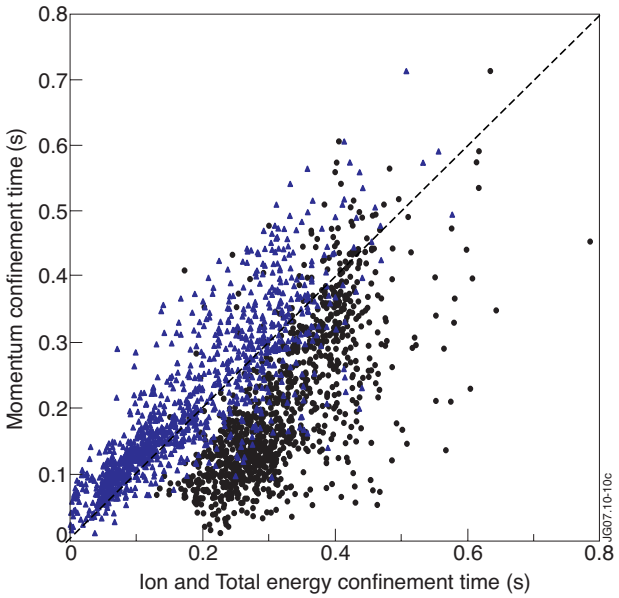

Figure 10: The momentum confinement time as a function of the ion energy replacement time (blue triangles) and the total energy confinement time (black dots). Determined for all types of discharges (Optimised Shear/ITB, L-mode, H-mode, Hybrid) in the period 2000-2004, with P_{NBI}*>6MW,* I_p*>2MA.*